Modulation of Butyrate Anticancer Activity by Solid Lipid Nanoparticle Delivery: An in Vitro Investigation on Human Breast Cancer and Leukemia Cell Lines

Federica Foglietta[a*], Loredana Serpe[a], Roberto Canaparo[a], Nicoletta Vivenza[b], Giovanna Riccio[b], Erica Imbalzano[a], Paolo Gasco[b], Gian Paolo Zara[a]

[a]Dipartimento di Scienza e Tecnologia del Farmaco, University of Torino, Torino, Italy. [b]Nanovector srl, Environment Park, Torino, Italy

Received, February 19, 2014; Revised, May 17, 2014; Accepted, May 21, 2014; Published, May 25, 2014.

ABSTRACT - Purpose. Histone modification has emerged as a promising approach to cancer therapy. The short-chain fatty acid, butyric acid, a histone deacetylase (HD) inhibitor, has shown anticancer activity. Butyrate transcriptional activation is indeed able to withdraw cancer cells from the cell cycle, leading to programmed cell death. Since butyrate's clinical use is hampered by unfavorable pharmacokinetic and pharmacodynamic properties, delivery systems, such as solid lipid nanoparticles (SLN), have been developed to overcome these constraints. **Methods.** In order to outline the influence of butyrate delivery on its anticancer activity, the effects of butyrate as a free (sodium butyrate, NB) or nanoparticle (cholesteryl butyrate solid lipid nanoparticles, CBSLN) formulation on the growth of different human cancer cell lines, such as the promyelocytic leukemia, HL-60, and the breast cancer, MCF-7 was investigated. A detailed investigation into the mechanism of the induced cytotoxicity was also carried out, with a special focus on the modulation of HD and cyclin-dependent kinase (CDK) mRNA gene expression by real time PCR analysis. **Results.** In HL-60 cells, CBSLN induced a higher and prolonged expression level of the butyrate target genes at lower concentrations than NB. This led to a significant decrease in cell proliferation, along with considerable apoptosis, cell cycle block in the G0/G1 phase, significant inhibition of total HD activity and overexpression of the p21 protein. Conversely, in MCF-7 cells, CBSLN did not enhance the level of expression of the butyrate target genes, leading to the same anticancer activity as that of NB. **Conclusions.** Solid lipid nanoparticles were able to improve butyrate anticancer activity in HL-60, but not in MCF-7 cells. This is consistent with difference in properties of the cells under study, such as expression of the *TP53* tumor suppressor, or the transporter for short-chain fatty acids, *SLC5A8*.

INTRODUCTION

Butyric acid is the main short-chain fatty acid (SCFA) produced by bacterial fermentation of dietary fiber in the colon. It is well known that butyrate plays an important role in the homeostasis of colonic mucosa by inducing pathways for cell maturation, as well as cell cycle arrest, differentiation and apoptosis (1). Butyrate-mediated regulation of apoptotic pathways also occurs in cancer cells, including myeloid leukemia and breast cancer cells, and is not limited to the gastrointestinal tract (2-4). Transcription is the primary target of butyrate, since it causes histone hyperacetylation through non-competitive and reversible inhibition of histone deacetylase (HD).

Butyrate enables DNA binding of several transcription factors, leading to higher genomic activity (5, 6). Apoptosis induced by histone deacetylase inhibitors (HDI) is generally associated with various disarrays of cell signaling pathways (7). Indeed, various studies have demonstrated the importance of epigenetic alteration, leading to gene silencing or abnormal expression as a cancer hallmark, and have proposed 'epigenetic' therapies capable of controlling transcription, as a promising approach in cancer therapeutics (8-10). The efficacy of HDI in cancer therapy may well stem from their restoration of silenced gene expression.

Corresponding Author: Federica Foglietta, Dipartimento di Scienza e Tecnologia del Farmaco, Università di Torino, Via Pietro Giuria 13, 10125 Torino, Italy; Email federica.foglietta@unito.it

One such example is the fact that the powerful tumor suppressor p53 is the most commonly inactivated protein in human tumors (11). Its inactivation may be the result of *TP53* gene alterations and approximately 50% of human cancers carry mutations in this gene (12).

It has now been well established that HDI treatment induces the expression of the cyclin-dependent kinase (CDK) inhibitor, p21. This plays a critical role in the regulation of cell cycle arrest and apoptosis, causing G1 arrest (13-16). HDIs have also been shown to induce p16 (CDKN2 or INK4) and p27, but they attenuate levels of cyclin A and cyclin D, leading to decreased CDK4 and CDK2 activity (17). HDI treatment triggers both the intrinsic pathway and sensitizes tumor cells to the extrinsic death ligand-induced pathway of apoptosis (17, 18). HDIs also have non-histone substrates and can modulate transcription by directly acetylating/deacetylating transcription factors, as well as associated cofactors such as Sp1 transcription factors or proteins, including p53 (19). Butyric acid seems to be particularly selective in regulating gene expression, leading to transcriptional activation of certain genes, such as *CDKN1A* coding p21 in a p53-independent manner (20, 21). However, although the precise molecular mechanism involved in the cancer therapeutics of butyric acid has not yet been fully clarified, it does seem to be highly dependent on the cellular context.

The clinical use of butyrate as an anticancer agent is hampered by unfavorable pharmacokinetic and pharmacodynamic properties. These include its short half-life, which requires administration of continuous parenteral infusions to maintain therapeutic concentrations (22, 23). By extension, factors affecting intracellular accumulation of butyrate could potentially influence its availability to modulate gene expression and, hence, processes such as proliferation, differentiation and apoptosis (24). Although free diffusion of fatty acids may take place, it has very little physiological relevance in the uptake of butyrate. There is now a considerable body of evidence suggesting that SCFAs are predominantly taken up via a facilitated process involving a number of transport proteins.

The relatively recent characterization of a number of trans-membrane proteins has led to two well-defined routes of uptake, both monocarboxylate transport proteins: MCT1 also known as SLC16A1, a hydrogen coupled transporter, and SMCT1 (SLC5A8), a sodium-coupled transporter (25). Thus, varying levels of transporter expression may result in a varied cellular uptake of butyrate. In particular, SLC5A8 is the first plasma membrane transporter postulated to function as a tumor suppressor (26). Silencing of its expression by epigenetic mechanisms is an early event in the progression of colorectal cancer and re-expression of the gene in colon tumor cell lines induces apoptosis and prevents colony formation (27, 28).

The newly developing field of nanomedicine offers very promising applications for nanotechnology as a drug delivery platform. The aim of nanomedicine can be broadly defined as the comprehensive monitoring, control, construction, repair, defense and improvement of all human biological systems, working from the molecular level using engineered devices and nanostructures, ultimately to achieve medical benefits. Thanks to their small size, nanoparticulate drug delivery systems are encouraging goals in cancer therapy approaches. These include selective or targeted drug delivery, enhanced drug transport across biological barriers (leading to an increased bioavailability of the entrapped drug) or intracellular drug delivery, which minimizes systemic side effects and improves the solubility of poorly water-soluble drugs (29). Thus, cholesteryl butyrate solid lipid nanoparticles (CBSLN) have been put forward as a special delivery system to improve butyrate anticancer activity. This is because they are also a pro-drug, with the lipid matrix of solid lipid nanoparticles made up of cholesteryl butyrate i.e. the ester of cholesterol and butyric acid (30, 32). Previous studies have shown that CBSLN are able to prevent premature degradation of the incorporated butyrate and enhance cell membrane crossing (including the blood-brain barrier) (33), oral bioavailability and anticancer efficacy (31, 34-36). Moreover, CBSLN have shown very low systemic toxicity (37, 38) as their matrix contains physiological components and/or excipients of accepted status (FDA-approved constituents) (39, 40). Thus, CBSLN as a butyrate drug delivery system might be a valuable anticancer tool, since it improves several aspects of butyrate pharmacology. However, to date, there have been no reports on the effects of CBSLN on butyrate anticancer activity at molecular level.

Our aim was to investigate the anticancer activity of butyric acid as a lipid nanoparticle formulation, with special attention to mRNA gene expression modulation in different human cancer cell lines such as the promyelocytic leukemia, HL-60, and the breast cancer, MCF-7.

MATERIALS AND METHODS

Cholesteryl butyrate solid lipid nanoparticles

CBSLN were prepared using the microemulsion method reported elsewhere (30, 31). Briefly, CBSLN were prepared from cholesteryl butyrate (0.54 mmol) (Asia Talent Chemical, Shenzen, China) and Epikuron 200 (0.66 mmol) (Cargill, Milan, Italy). Epikuron 200 and cholesteryl butyrate were melted at 85 °C and a warm solution of sodium glycocholate (0.39 mmol) (PCA, Basaluzzo, Italy) was added. 2-phenylethanol (Sigma Aldrich, Milan, Italy) was used as a preservative (0.25% w/v final dispersion). The microemulsion was then immediately dispersed in cold water (dispersion ratio 1:5 v/v) and washed by tangential flow filtration using a Vivaflow50 membrane (Sartorius Stedim Biotech GmbH, RC, Cut-off 100,000 Da) for purification of hydrophilic molecules (four washing steps were repeated by addition and removal of the same volume of water). The aqueous dispersion of CBSLN was then sterilized by 0.2 µm filtration before use. Dispersion of CBSLN was characterized according to average diameter (Zave) and polydispersity index (PI) (Photon Correlation Spectroscopy (PCS), Malvern Zetasizer - Nano ZS – 176 Deg) and by determination of chemical composition (HPLC-UV analysis, Agilent 1260 and 1200). The zeta potential of the chol-but CBSLN dispersion after final sterilizing filtration was also characterized by laser Doppler velocimetry (LDV) (Malvern Zetasizer - Nano ZS).

Fluo-cholesteryl butyrate SLN was prepared using the warm microemulsion method as for unlabeled CBSLN, by simply adding fluorescent dye in the lipid phase. Briefly, a warm microemulsion was prepared from cholesteryl butyrate (CBSLN 0.54 mmol), Epikuron 200 (PC) (0.66 mmol), 3,3'-dioctadecyloxacarbocyanine perchlorate (DiO, λex: 484 nm / λemiss: 501 nm) (Biotium, Hayward – USA) (0.9 µmol), as the lipid phase and sodium glycocholate (NaGC, 0.39 mmol) (PCA, Basaluzzo, Italy) in the water phase; 2-phenylethanol (PhOH) (Sigma Aldrich, Milan, Italy) was added as a preservative (0.25% w/v final dispersion). DiO-tagged CBSLN aqueous dispersion was washed and sterilized as for the previously reported unlabeled CBSLN.

Since the whole lipid matrix of CBSLN themselves acts as a prodrug of butyrate, solutions of sodium butyrate were freshly prepared in sterile water before each experiment and used as a drug reference.

Cell culture and proliferation assay

HL-60 and MCF-7 cell lines (ICLC, Interlabab Cell Line Collection, Genoa, Italy) were cultured in a growth medium (RPMI 1640 medium) supplemented with 2 mM L-glutamine, 100 UI/mL penicillin, 100 µg/mL streptomycin and 10% (v/v) heat-inactivated fetal calf serum (Sigma, St Louis, MO, USA) in a humidified atmosphere of 5% CO_2 air at 37 °C.

The effect of butyrate, as NB or CBSLN, on HL-60 and MCF-7 cell growth was evaluated by WST-1 cell proliferation assay (Roche Applied Science, Penzberg, Germany). 1×10^3 HL-60 and 2.5×10^3 MCF-7 cells were seeded in 100 µL of growth medium in replicates (n = 8) in a 96-well culture plate. After 72 h of cell growth, the medium was removed and the cells were incubated with the experimental medium containing different butyrate concentrations (0.01, 0.10, 0.50 and 1.00 mM). At 24 h and 48 h, WST-1 reagent (10 µL) was added and the plates were incubated at 37 °C in 5% CO_2 for 2 h. Well absorbance was measured at 450 nm and 620 nm (reference wavelength) in the Asys UV 340 microplate reader (Biochrom, Cambridge, UK). Cell proliferation data were expressed as a percentage of untreated cells.

Flow cytometry

Cell death was evaluated using the Dead Cell Apoptosis Kit with (allophycocyanin) APC-Annexin V and Sytox® Green (Life Technologies, Milan, Italy). Briefly, 5 x 10^5 HL-60 and MCF-7 cells were treated with butyrate (NB or CBSLN) 0.50 mM and 1.00 mM, respectively. The cells were then washed twice with 1x annexin-binding buffer at 375 rcf for 5 min and were stained with APC-Annexin V and Sytox® Green at 12, 24 and 48 h. Samples were run on the flow cytometer at a 640 nm excitation to measure APC-Annexin V (FL4) and at 488 nm to measure Sytox® Green (FL1), respectively. Any cell debris with low FSC and SSC was excluded from the analyses. A total of 10,000 events were analyzed for APC-Annexin V (FL4) and Sytox® Green (FL1) staining to discriminate apoptotic (Annexin V positive) or late apoptotic/necrotic cells (Annexin V and Sytox® Green positive) from viable cells (Annexin V and Sytox® Green negative).

Cell cycle distribution was monitored by adding 2 µM of Vybrant Dye Cycle Green (Invitrogen) live cell staining to 10^6 cells for 30 min at 37 °C. Briefly, both the HL-60 and the MCF-7 cell cycle distributions were evaluated after the treatment with butyrate (NB or CBSLN) 0.50 mM at 12 h and 1.00

mM at 48 h, respectively. The samples were run on the flow cytometer with a 488 nm excitation to measure the Vybrant Dye Cycle Green staining (FL2). Flow cytometry was carried out by a C6 flow cytometer (Accurri Cytometers, Milan, Italy) and the analysis was performed by a FCS Express 4 (BD Bioscience, Milan, Italy).

Cellular uptake studies of CBSLN were carried out by flow cytometry with 3,3'-dioctadecyloxacarbocyanine perchlorate (DiO) used as a fluorescence probe. The experiment was conducted on 1×10^5 cells in a six-well culture plate. Cells were incubated at 37 °C, 5% CO_2 in supplemented RPMI-1640 medium. Then, HL-60 and MCF-7 cells were treated with 1 mL of 0.50 mM of DiO-tagged CBSLN in RPMI-1640 medium for 1, 5, 15, 30 and 60 min. After each incubation period, the cells were washed three times with PBS, and re-suspended in 300 µl PBS and run on the flow cytometer with a 488 nm excitation to measure the DiO staining (FL1). Intracellular fluorescence was expressed as the integrated median fluorescence intensity (iMFI), which was the product of the frequency of DiO-tagged CBSLN positive cells and the median fluorescence intensity of the cells. Results were expressed as the iMFI ratio, i.e. the difference between the iMFI of treated and untreated cells and the iMFI of untreated cells (41).

Fluorescence microscopy

HL-60 and MCF-7 cellular uptake of 3,3'-dioctadecyloxacarbocyanine perchlorate (DiO)-tagged CBSLN was investigated by fluorescence microscopy. Briefly, the MCF-7 cells were left to attach for 24 h on glass coverslips in 24-well plate, 2 x 10^5 HL-60 and MCF-7 cells were then incubated for 30 min with DiO-tagged CBSLN 0.50 mM. Five minutes before the programmed stop time, the cells were incubated with 1 µg/mL of 4',6-diamidino-2-phenylindole (DAPI) for nuclear staining. Once the cells had been washed with PBS, the HL-60 cell suspensions and the MCF-7 on the coverslip were mounted onto a glass slide, observed under a DMI4000B fluorescence microscope (Leica, Wetzlar, Germany) and photographed. A total of 50 cells per slide were analyzed at 40x magnification in three separate areas, three times in three individual experiments.

Real Time RT-PCR

Depending on the effects obtained on cell growth, total RNA was isolated from the HL-60 cells at 6 and 12 h after NB or CBSLN 0.50 mM treatment and from the MCF-7 cells at 24 and 48 h after NB or CBSLN 1.00 mM treatment. Briefly, HL-60 and MCF-7 cells were collected in an RNA Cell Protection Reagent (Qiagen, Milan, Italy) and stored at -80 °C. Total RNA was then obtained using the RNeasy Plus Mini Kit (Qiagen). The total RNA concentration (µg/mL) was determined using the Qubit fluorometer (Invitrogen, Milan, Italy) and the Quant-IT RNA Assay Kit (Invitrogen) was used. Calibration was performed applying a two-point standard curve, according to the manufacturer's instructions. The integrity of the RNA samples was determined using the total RNA 6000 Nano Kit (Agilent Technologies, Milan, Italy) and the Agilent 2100 Bioanalyzer (Agilent Technologies).

Real-time RT-PCR analysis was carried out using 500 ng of total RNA, which was reverse transcribed in a 20 µL cDNA reaction volume using the QuantiTect Reverse Transcription Kit (Qiagen). In accordance with the manufacturer's instructions, 12.5 ng of cDNA was used for each 10 µL real-time RT-PCR reaction. Quantitative RT-PCR was performed using SsoFast EvaGreen (Bio-Rad, Milan, Italy) and the QuantiTect Primer Assay (Qiagen) was used as the gene-specific primer pair for the panel of genes studied (Table 1). The transcript of the reference glyceraldehyde-3-phosphate dehydrogenase gene (*GAPDH*) was used to normalize mRNA data and real-time PCR was performed using a MiniOpticon Real Time PCR system (Bio-Rad). The PCR protocol conditions were as follows: HotStarTaq DNA polymerase activation step at 95 °C for 30 s, followed by 40 cycles at 95 °C for 5 s and 55 °C for 10 s. All runs were performed with at least three independent cDNA preparations per sample and all samples were run in duplicate. At least two non-template controls were included in all PCR runs. The quantification data analyses were performed using the Bio-Rad CFX Manager Software version 1.6 (Bio-Rad) according to the manufacturer's instructions. These analyses were performed in compliance with MIQE guidelines (Minimum Information for Publication of Quantitative Real-time PCR Experiments) (42).

HD activity quantification

Depending on the effects on cell growth, the HL-60 cells were collected at 12 h after NB or CBSLN 0.50 mM treatment and the MCF-7 cells at 48 h after NB or CBSLN 1.00 mM treatment.

Table 1. Gene description

Gene	Primers code	Description
AKT1	QT00085379	Protein kinase B
APAF1	QT00092358	Apoptotic peptidase activating factor 1
BAX	QT00062090	Pro-apoptosis regulator
BCL2	QT00031192	Anti-apoptosis regulator
CDK2	QT00005586	Cyclin-dependent kinase 2
CDK4	QT00016107	Cyclin-dependent kinase 4
CDKN1A	QT00031192	Cyclin-dependent kinase inhibitor 1A, p21
CDKN2A	QT00089964	Cyclin-dependent kinase inhibitor 2A, p16
GAPDH	QT01192646	Glyceraldehyde-3-phosphate dehydrogenase
HDAC1	QT00015239	Histone deacetylase 1
HDAC2	QT00001890	Histone deacetylase 2
HDAC4	QT00005810	Histone deacetylase 4
MAP3K15	QT00041594	Member of the mitogen-activated protein kinase
NFKB1	QT00063791	Nuclear factor kappa-B DNA binding subunit
SLC5A8	QT00199367	Sodium-coupled monocarboxylate transporter 1
SLC16A1	QT00060676	Solute carrier family 16 member 1
TP53	QT00060235	Tumor suppressor protein, p53

In order to evaluate deacetylation by HD enzymes, nuclear extracts were prepared using the Nuclear Extract Kit (Active Motif, Rixensart, Belgium) to obtain the nuclear proteins, starting from 3 x 10^6 cells.

The protein concentration (µg/mL) was quantified using the Qubit fluorometer and the Quant-IT Protein Assay Kit. Calibration was performed applying a two-point standard curve, according to the manufacturer's instructions. We then used the colorimetric HD Assay Kit (Active Motif) according to the manufacturer's instructions. This colorimetric HD assay uses a short peptide substrate containing an acetylated lysine residue that can be deacetylated by class I, II and IV HD enzymes. Well absorbance was measured at 405 nm in the microplate reader Asys UV 340.

p21 protein quantification

HL-60 cells were collected at 12 h after NB or CBSLN 0.50 mM treatment and the MCF-7 cells at 48 h after NB or CBSLN 1.00 mM treatment. 1 x 10^6 cells were washed twice with PBS, collected in PBS and stored at -80 °C. The p21 in the cell lysates was analyzed using the p21 EIA kit (Enzo Life Sciences, Milan, Italy) according to the manufacturer's instructions. The protein concentration (µg/mL) was quantified using the Qubit fluorometer and the Quant-IT Protein Assay Kit. Calibration was performed applying a two-point standard curve, according to the manufacturer's instructions.

STATISTICAL ANALYSIS

Data are shown as the mean values ± SD of three independent experiments. Statistical analyses were performed with GraphPad Prism 6.0 software (La Jolla, CA, USA) using the analysis of variance (two-way ANOVA). Bonferroni's test was used to calculate the threshold of significance. Statistical significance was set at $P < 0.05$.

RESULTS

Characterization of cholesteryl butyrate solid lipid nanoparticles

The average diameter (Zave) and polydispersity index (PI) of CBSLN after 0.2 µm filtration were 78.13 nm and 0.240, respectively. The concentration of cholesteryl butyrate and consequently of butyrate, determined by reversed-phase HPLC after washing four times, were 38.6 mM and 38.6 mM, respectively and, after 0.2 µm filtration, 36 mM and 36 mM, respectively.

Effects of SLN butyrate delivery on cell proliferation

CBSLN were observed to enhance butyrate antiproliferative activity in HL-60 cells but not in MCF-7 cells, as shown in Figure 1. In HL-60 cells, CBSLN determined a significant dose-dependent decrease in cell proliferation starting from 24 h of exposure, whereas NB induced only a slight reduction in cell proliferation at 48 h of exposure to

the highest concentration tested (1.00 mM). In MCF-7 cells, CBSLN did not enhance the cytotoxic effects of butyrate, since it determined the same NB activity with a significant decrease in cell proliferation starting from 24 h of exposure to the highest concentration tested (1.00 mM). CBSLN were able to increase butyrate activity in leukemic cells but not in breast cancer cells, as compared to free butyrate.

Effects of SLN butyrate delivery on cell death

On the basis of cell proliferation data (Figure 1), HL-60 cell death was evaluated at 12, 24 and 48 h of exposure to 0.50 mM NB or CBSLN. At 0.50 mM, CBSLN induced a significant increase in the percentage of apoptotic and necrotic cells, which reached 50% and 30%, respectively of the whole cell population at 12 h. The increase in apoptotic and necrotic cell percentage was maintained for up to 48 h after treatment (Figure 2). Conversely, 0.50 mM NB induced an increase in the apoptotic cell percentage which reached about 30% of the whole cell population only at 48 h (Figure 2). On the basis of cell proliferation data, MCF-7 cell death was evaluated at 24 and 48 h after 1.00 mM NB or CBSLN treatment. A slight increase in the apoptotic cell percentage was detectable only at 48 h with NB treatment, while the same formulation did not induce a significant increase in the percentage of necrotic cells (Figure 2). These data demonstrate that CBSLN were able to induce a significant increase in apoptotic and necrotic cell percentage, compared to free butyrate, at 12 h, while CBSLN were not able to improve necrotic or apoptotic cell death in MCF-7 cells.

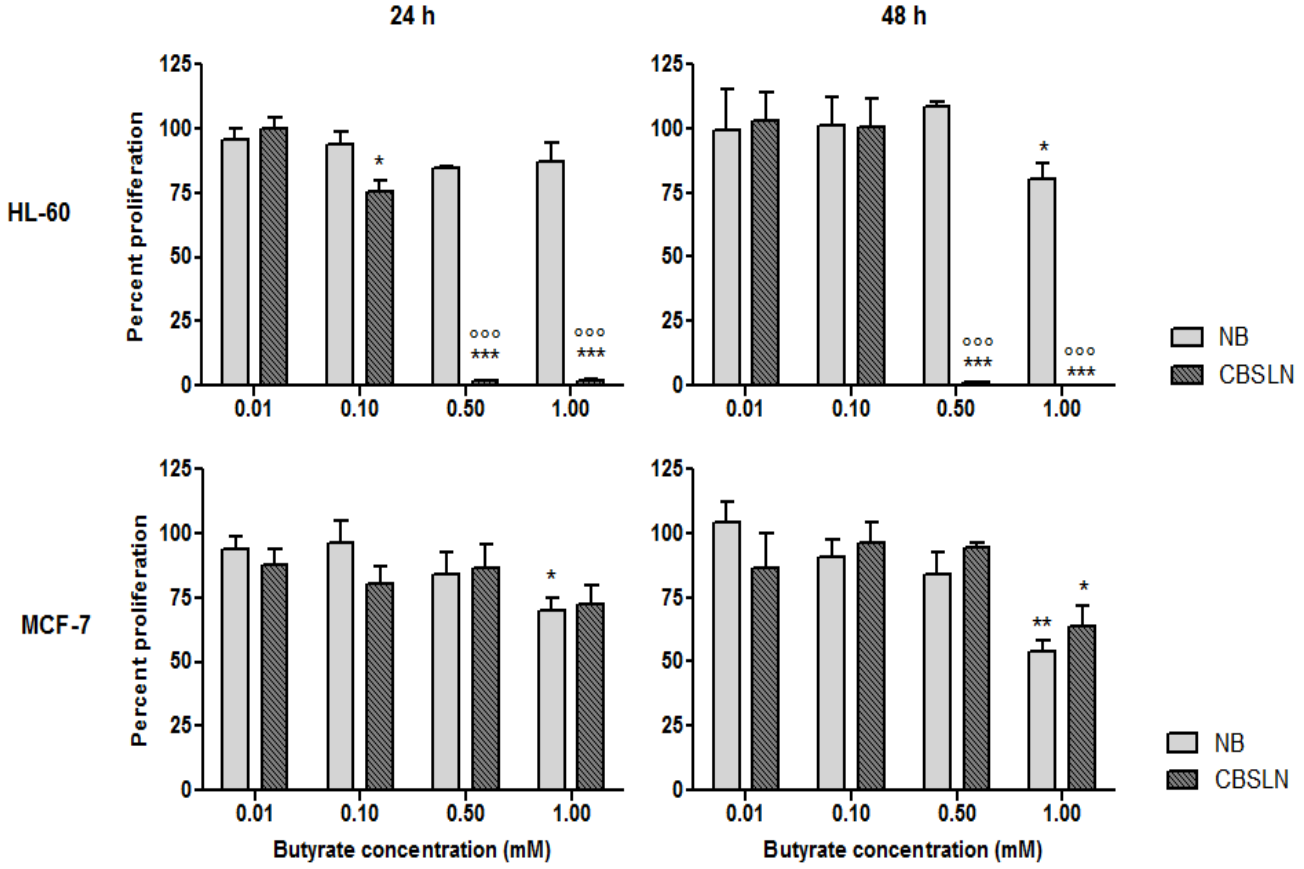

Figure 1. Effects of SLN butyrate delivery on cell proliferation. HL-60 and MCF-7 cell proliferation after exposure to increasing concentrations of butyrate as NB or CBSLN was evaluated at 24 and 48 h by WST-1 assay. Data are expressed as a percentage of control cells, i.e. untreated cells (100%). * $P < 0.05$, ** $P < 0.01$, *** $P < 0.001$ statistical significance versus control cells; °°° $P < 0.001$ statistical significance versus NB treated cells.

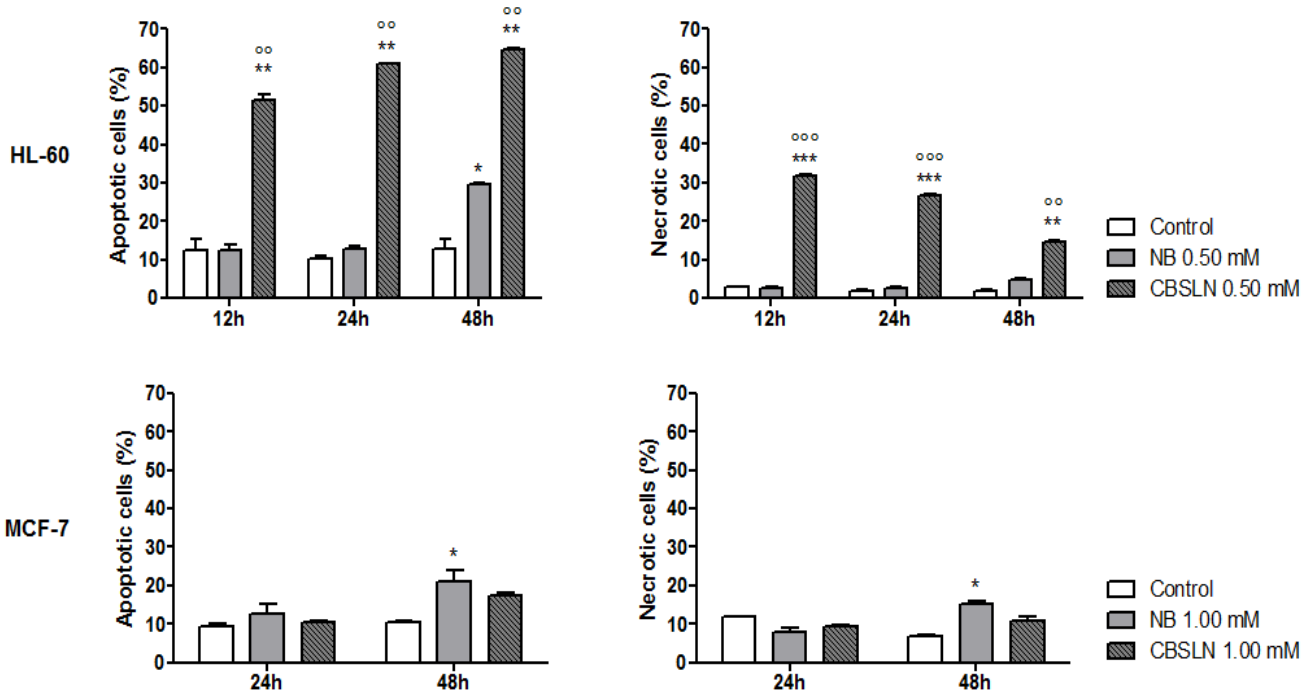

Figure 2. Effects of SLN butyrate delivery on cell death. Percentages of apoptotic and necrotic cells were obtained by flow cytometry with APC-Annexin V and Sytox Green for HL-60 at 12, 24 and 48 h exposure to 0.50 mM NB or CBSLN and for MCF-7 at 24 and 48 h exposure to 1.00 mM NB or CBSLN. * $P < 0.05$, ** $P < 0.01$, *** $P < 0.001$ statistical significance versus control cells; °° $P < 0.01$, °°° $P < 0.001$ statistical significance versus NB treated cells.

Effects of SLN butyrate delivery on cell cycle distribution

The lowest butyrate concentrations able to influence cell proliferation, i.e. 0.50 mM for HL-60 cells and 1.00 mM for MCF-7 cells (Figure 1), were evaluated for their effects on cell cycle distribution. Owing to the severe decrease in HL-60 cell viability after 0.50 mM CBSLN treatment, cell cycle distribution was only evaluated at 12 h of incubation. A statistically significant difference in the percentage of HL-60 cells in each cell cycle phase was observed after exposure to 0.50 mM CBSLN compared to both untreated and NB treated cells (Table 2). At 0.50 mM, CBSLN showed a statistically significant increase in HL-60 cells in the G0/G1 phase and a reduction in the S and G2/M phases, which was compatible with an arrest in the G0/G1 phase (Table 2). However, little difference was observed, in both 1.00 mM NB and CBSLN treated cells, in the proportion of MCF-7 cells in any cell cycle phase (Table 2). Thus, CBSLN were able to increase butyrate activity on the leukemic cell cycle, while the two butyrate formulations had similar effects on the breast cancer cell cycle.

CBSLN cellular uptake

Since differences in growth, death and cell cycle distribution were observed between HL-60 and MCF-7 cells exposed to the same CBSLN concentrations, their cellular uptake was investigated first by means of fluorescence microscopy. Both the HL-60 and MCF-7 cells seemed to have internalized the DiO-tagged CBSLN 0.50 mM after 30 min of incubation in more than 80% of the whole cell population (Figure 3a and b).

In order to explore the DiO-tagged CBSLN internalization, a flow cytometric analysis was performed. Specifically, leukemia cells were able to internalize DiO-tagged CBSLN 0.50 mM with a high iMFI ratio 1 min after incubation, reaching maximum internalization at 30 min ($P < 0.001$). The MCF-7 DiO-tagged CBSLN uptake was slower and almost constant during the time of incubation (Figure 3c). These data showed that the CBSLN internalization rate was higher and the kinetic uptake was faster in leukemia cells than in breast cancer cells.

Table 2. Effects of SLN butyrate delivery on cell cycle distribution

Butyrate	mM	HL-60 cells (%) at 12 h exposure			nM	MCF-7 cells (%) at 48 h exposure		
		G0/G1	S	G2/M		G0/G1	S	G2/M
Control	0	31.5 ± 2.5	41.6 ± 5.2	26.8 ± 3.1	0	52.5 ± 4.6	37.9 ± 3.2	9.5 ± 1.3
NB	0.50	34.5 ± 4.1	45.9 ± 4.3	19.4 ± 2.7	1.00	47.3 ± 3.6	32.4 ± 4.5	12.7 ± 3.2
CBSLN	0.50	85.1 ± 4.2***	10.8 ± 2.1***	4.3 ± 0.7***	1.00	51.7 ± 6.4	34.8 ± 5.6	10.7 ± 2.7

Notes: *** $P < 0.001$ statistical significance versus control cells

Effects of SLN butyrate delivery on gene expression

Based on the cell proliferation data (Figure 1), HL-60 RNA was extracted at 6 and 12 h after 0.50 mM NB or CBSLN treatment and MCF-7 RNA was extracted at 24 and 48 h after 1.00 mM NB or CBSLN treatment. HL-60 samples (n = 18) had an RNA integrity number (RIN) of 10.00 ± 0.00 and MCF-7 samples (n = 18) had an RIN of 9.95 ± 0.05. The fold change in mRNA expression levels of genes involved in the butyrate mechanism of action, as compared to the control cells, i.e. untreated cells (expression level = 1), is reported for HL-60 cells in Figure 4 and for MCF-7 cells in Figure 5.

We analyzed the gene expression profile of HL-60 at 6 and 12 h after 0.50 mM NB (Figure 4a) or CBSLN (Figure 4b) treatment. Of note is that the *TP53* gene was not expressed in the HL-60 cell line (Figure 4a and b). No significant modifications was observed in the mRNA expression of the HD genes of class I, i.e. *HDAC1* and *2* (Figure 4a and b). Conversely, the HD gene of class II, *HDAC4*, was significantly over-expressed at 12 h after CBSLN treatment (Figure 4b).

As it is well known that butyrate is able to induce cell cycle arrest and apoptosis, we analyzed the expression levels of some genes involved in these pathways.

CDK4, which regulates the cell cycle during G1/S transition, was slightly over-expressed at 6 h after NB (Figure 4a) and 12 h after CBSLN treatment (Figure 4b). Furthermore, the mRNA expression level of *CDKN2A*, which codes for the CDK4 inhibitor p16, was increased at 6 h after NB treatment (4.8 ± 0.1, Figure 4a) and, to a greater extent, at 12 h after CBSLN treatment (9.8 ± 0.2, Figure 4b). *CDKN1A*, which codes for the CDK inhibitor p21 – characterized by a specific sequence on its promoter region recognized by butyrate – was significantly over-expressed both at 6 and 12 h after NB (Figure 4a) and CBSLN treatment (Figure 4b). The highest mRNA expression level of *CDKN1A* was observed at 12 h after CBSLN treatment (64.00 ± 5.00, Figure 4b). This expression profile was in line with the considerable G0/G1 block and apoptosis observed in HL-60 cells after 0.50 mM CBSLN treatment (Table 2 and Figure 2). As treatment with HDI triggers cancer cells in both the extrinsic and intrinsic death ligand-induced pathways for apoptosis, we also analyzed genes such as *AKT1* and *APAF1*. Specifically, it was observed that, *AKT1*, which is involved in the transduction pathway of the tyrosine-kinase receptor, was significantly over-expressed at 6 h after NB treatment (Figure 4a) and at 12 h after CBSLN treatment (Figure 4b). *APAF1*, which mediates the cytochrome c-dependent autocatalytic activation of pro-caspase-9, was significantly over-expressed at 6 h after NB treatment (Figure 4a) and at 12 h after CBSLN treatment (Figure 4b). When the pro-apoptotic *BAX* gene and the anti-apoptotic *BCL-2* gene were taken into consideration, no statistically significant differences were observed in the mRNA expression levels, either after NB (Figure 4a) or after CBSLN (Figure 4b) treatment. Furthermore, the expression of *MAP3K15* and *NFKB1* gene encoding transcriptional factors, which play an essential role in apoptotic cell death triggered by cellular stresses, was affected by neither butyrate, NB (Figure 4a) nor CBSLN (Figure 4b) treatment. The expression levels of two genes, *SLC5A8* and *SLC16A1* encoding butyrate transporters were also analyzed. There was no *SLC5A8* expression in HL-60 cells (Figure 6a and b), whilst the mRNA expression level of *SLC16A1* remained unaffected by butyrate both as NB (Figure 6a) and as CBSLN (Figure 6b).

We analyzed the MCF-7 gene expression profile at 24 and 48 h after 1.00 mM NB (Figure 5a) or CBSLN (Figure 5b) treatment. Noteworthy is the fact that the *TP53* gene in the MCF-7 cell line was expressed and differentially modulated by NB and CBSLN at 24 h, reaching control level at 48 h (Figure 5a and b). *HDAC1*, *2* and *4* were down-expressed at 24 h and over-expressed at 48 h by NB (Figure 5a). Conversely, these genes were over-expressed at 24 h and down-expressed at 48 h after CBSLN treatment (Figure 5b).

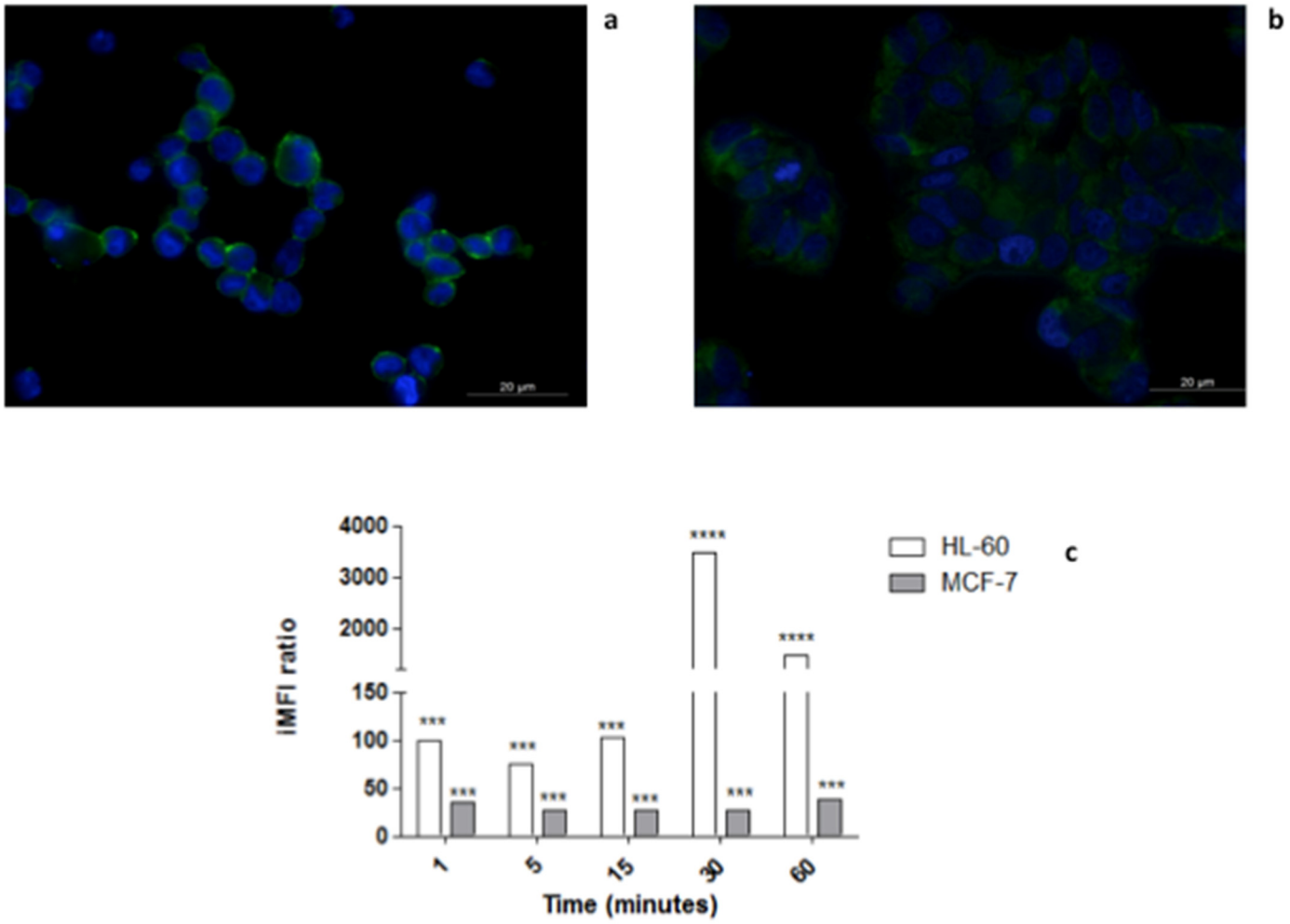

Figure 3. CBSLN cellular uptake. Figure a: Representative fluorescence image of HL-60 cells exposed to 0.50 mM 3,3'-dioctadecyloxacarbocyanine perchlorate (DiO)-tagged cholesteryl butyrate solid lipid nanoparticles (CBSLN) (in green) for 30 min; DAPI (in blue) was used as nuclear counterstain, at 63x magnification. Figure b: Representative fluorescence image of MCF-7 cells exposed to 0.50 mM DiO-tagged CBSLN (in green) for 30 min; DAPI (in blue) was used as nuclear counterstain, at 63x magnification. Figure c: Cellular uptake by flow cytometric analysis, cells was exposed to DiO-tagged CBSLN for different incubation time (1, 5, 15, 30, 60 min). Fluorescent signal was detected by a flow cytometer with a 488 nm excitation to measure the DiO staining (FL1) and expressed as integrated median fluorescence intensity (iMFI) ratio calculated as reported in Materials and Methods. *** $P < 0.001$, ****$P < 0.0001$ statistical significance versus untreated cells.

mRNA expression levels of *CDK2* and *CDK4* had significantly decreased at 24 h after NB reaching control level at 48 h (Figure 5a). CBSLN modulated *CDK2* expression only at 24 h (Figure 5b). Although *CDKN2A* was down-regulated by both NB and CBSLN at 48 h, CBSLN treatment led to an up-regulation at 24 h (Figure 5a and b). *CDKN1A* was similarly modulated by NB and CBSLN reaching the same extent of over-expression at 48 h (Figure 5a and b). Moreover, *AKT1* was down- regulated at 48 h by NB and CBSLN treatment, as was *NFKB1*, whilst *BAX* was slightly over-expressed (Figure 5a and b). Regarding the expression of the butyrate transporter genes, at 48 h we observed over-expression of *SLC5A8* after NB treatment and over-expression of *SLC16A1* after CBSLN treatment (Figure 6c and d).

Effects of SLN butyrate delivery on HD activity

Data are expressed as the HD activity fold change compared to control cells, i.e., untreated cells. HD activity was 235.27 ± 36.71 nmol/min/mg in untreated HL-60 cells and 192.97 ± 25.42 nmol/min/mg in untreated MCF-7 cells.

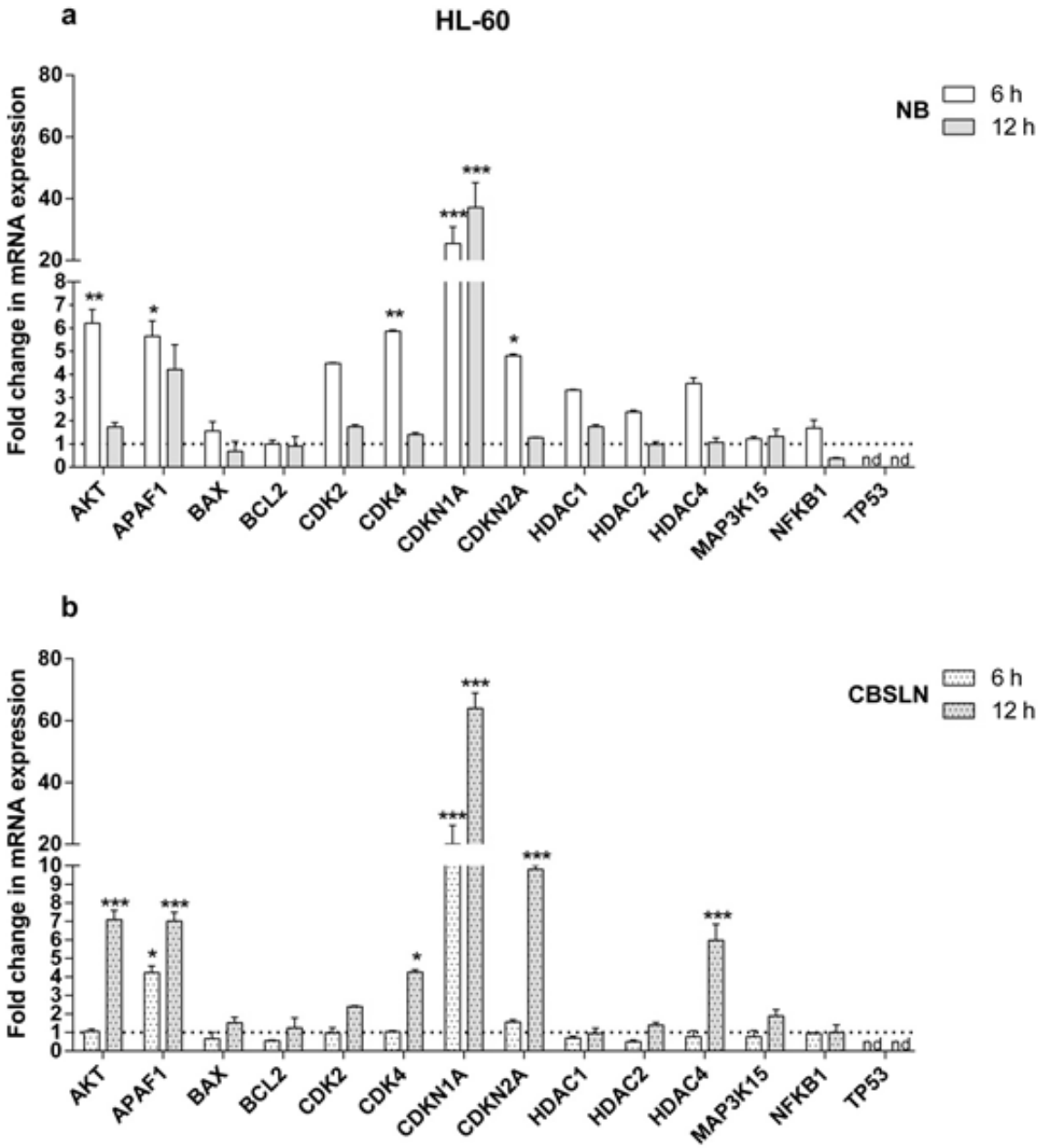

Figure 4. Effects of SLN butyrate delivery on HL-60 mRNA expression. mRNA gene expression was evaluated by real-time RT-PCR at 6 and 12 h from treatment with 0.50 mM of butyrate as NB (a) or CBSLN (b). Values are relative to untreated cells represented as the dash line, i.e. a value of 1; nd: not detectable; * $P < 0.05$, ** $P < 0.01$, *** $P < 0.001$ statistical significance versus untreated cells.

There was a significant reduction in total HL-60 HD activity after 12 h of exposure to 0.50 mM CBSLN, while NB had no effect (Figure 7a). Conversely, there was a slight decrease in the HD activity of MCF-7 nuclear extract samples after 48 h of exposure to 1.00 mM NB, while CBSLN had no effect (Figure 7b).

These alterations in total HD activity are consistent with the *HDAC4* mRNA over-expression observed in HL-60 cells at 12 h of exposure to 0.50 mM CBSLN (Figure 4b) and in MCF-7 cells at 48 h of exposure to 1.00 mM NB (Figure 5a), suggesting some kind of compensatory feedback (40).

Effects of SLN butyrate delivery on p21 protein expression

Data are expressed as the p21 protein expression fold change compared to control cells, i.e., untreated cells. The p21 protein was 2626.67 ± 158.41 pg/mL in untreated HL-60 cells and 4760.00 ± 310.03

pg/mL in untreated MCF-7 cells. A significant increase in p21 protein expression was observed in HL-60 cells after 12 h of exposure to 0.50 mM CBSLN (Figure 8a), in line with the marked *CDKN1A* mRNA over-expression observed (Figure 4b). Conversely, there was no difference in the MCF-7 p21 protein expression as compared to control cells after either NB, or CBSLN treatment (Figure 8b). This finding is in line with the slight increase in *CDKN1A* mRNA expression observed in MCF-7 cells after treatment with 1.00 mM NB or after CBSLN treatment (Figure 5a and b).

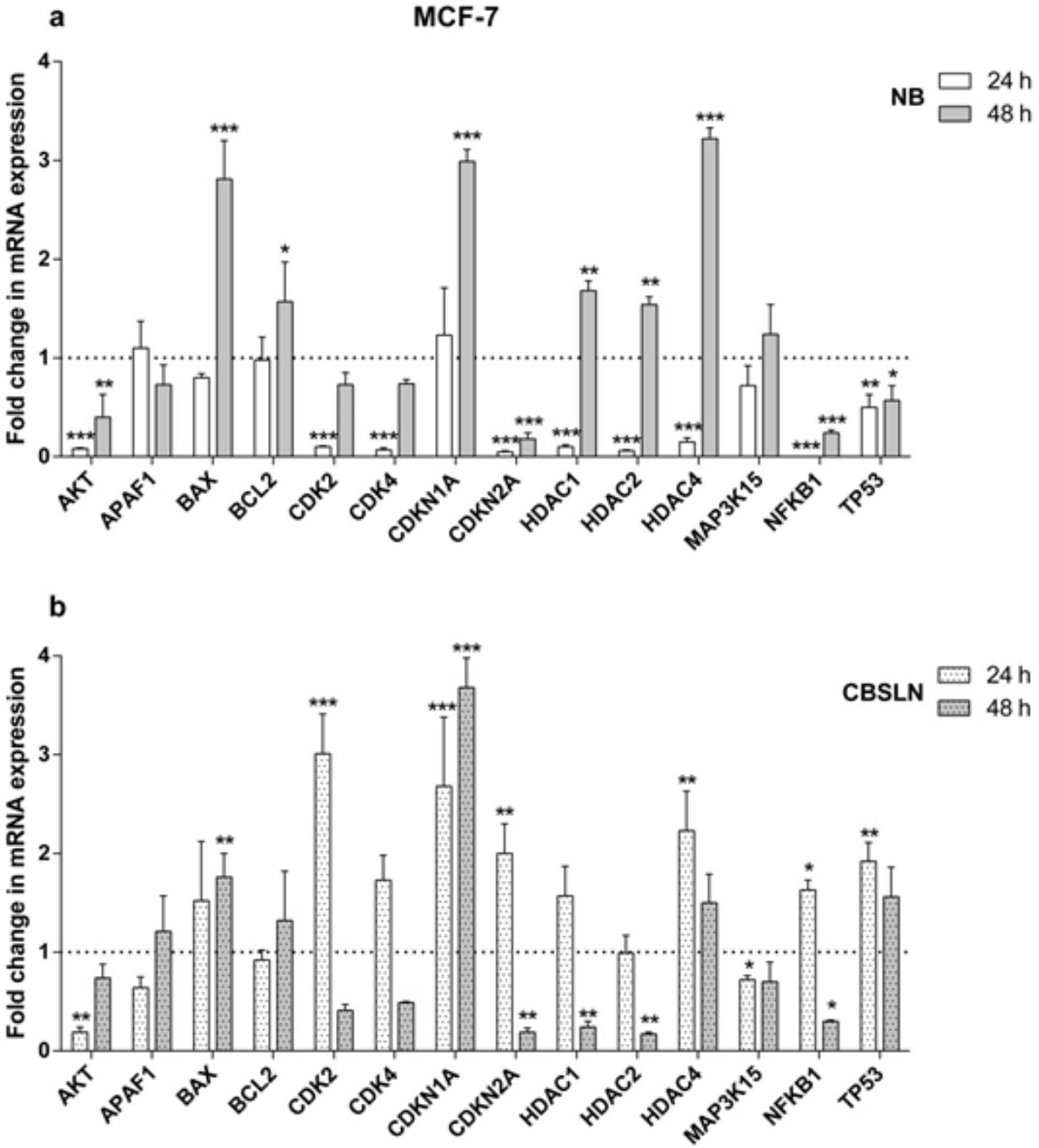

Figure 5. Effects of SLN butyrate delivery on MCF-7 mRNA expression. mRNA gene expression was evaluated by real-time RT-PCR at 24 and 48 h from the treatment with 1.00 mM of butyrate as NB (a) or CBSLN (b). Values are relative to untreated cells represented as the dash line, i.e. a value of 1; nd: not detectable; * $P < 0.05$, ** $P < 0.01$, *** $P < 0.001$ statistical significance versus untreated cells.

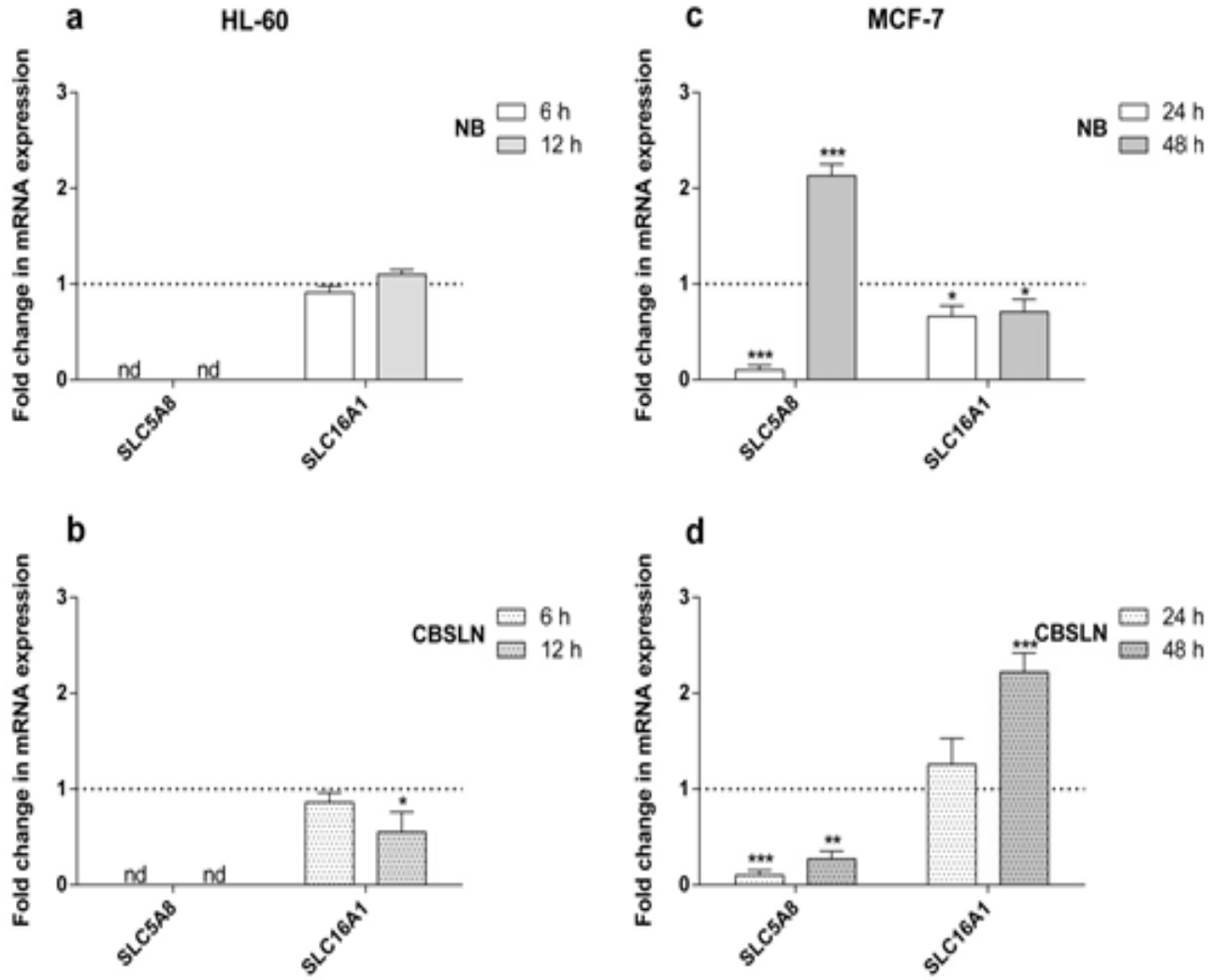

Figure 6. Effects of SLN butyrate delivery on mRNA expression of butyrate transporter genes. HL-60 mRNA gene expression was evaluated by real-time RT-PCR at 6 and 12 h from the treatment with 0.50 mM of butyrate as NB (a) or CBSLN (b). MCF-7 mRNA gene expression was evaluated by real-time RT-PCR at 24 and 48 h from the treatment with 1.00 mM of butyrate as NB (c) or CBSLN (d). Values are relative to untreated cells represented as the dash line, i.e. a value of 1; nd: *SLC5A8* gene expression not detectable in HL-60. * $P < 0.05$, ** $P < 0.01$, *** $P < 0.001$ statistical significance versus untreated cells.

DISCUSSION

Solid lipid nanoparticles are able to improve not only the pharmacokinetic, but also the pharmacodynamic properties of anti-cancer agents (39, 40, 43-45). Butyrate induces apoptosis and blocks in the G0/G1 phase in most cell lines at concentrations from 2 to 5 mM (14, 46, 47). Therefore, we investigated how solid lipid nanoparticles may influence the butyrate anticancer activity at a molecular level. CBSLNswere able to improve *in vitro* butyrate anticancer activity at lower concentrations in HL-60, but not in MCF-7 cells (Figure 1-2 and Table 2). These data are confirmed by the cellular uptake of fluorescent CBSLN, which was significantly higher in HL-60 than in MCF-7.

It is reasonable to suppose that the form of endocytosis involved in nanoparticle uptake could affect both intracellular localization and trafficking of the nanoparticles. To the best of our knowledge, differences in uptake extent and mechanism by hematological and epithelial cancer cell lines have not been reported to date. This is in spite of the fact that nanoparticles have been shown to exploit more than one pathway in their attempt to gain cellular entry (45).

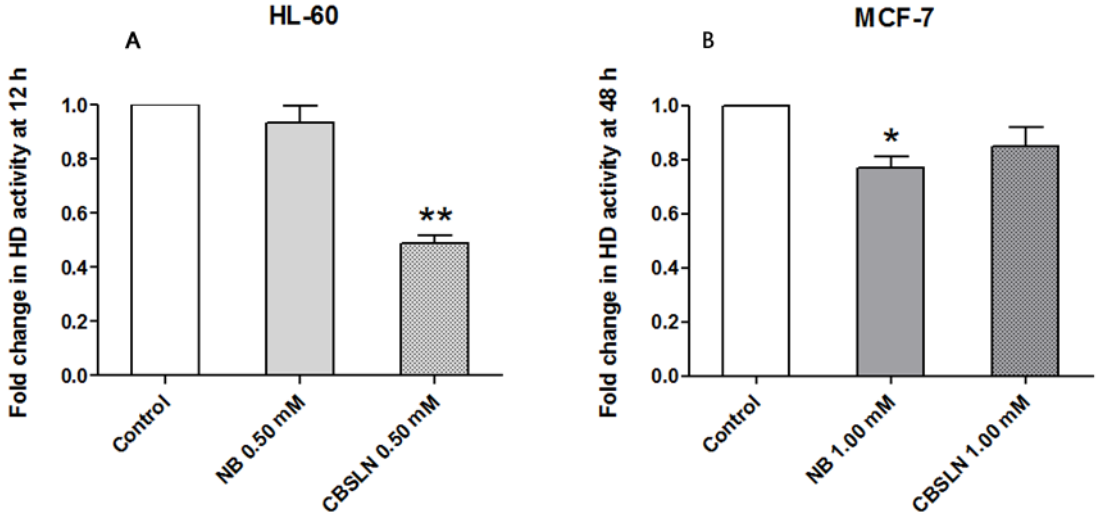

Figure 7. Effects of SLN butyrate delivery on HD activity. Data are presented as fold change compared to that of control cells, i.e. untreated cells. HD activity in untreated HL-60 cells was 235.27 ± 36.71 nmol/min/mg (a) and in untreated MCF-7 cells 192.97 ± 25.42 nmol/min/mg (b). * $P < 0.05$, ** $P < 0.01$ statistical significance versus control cells.

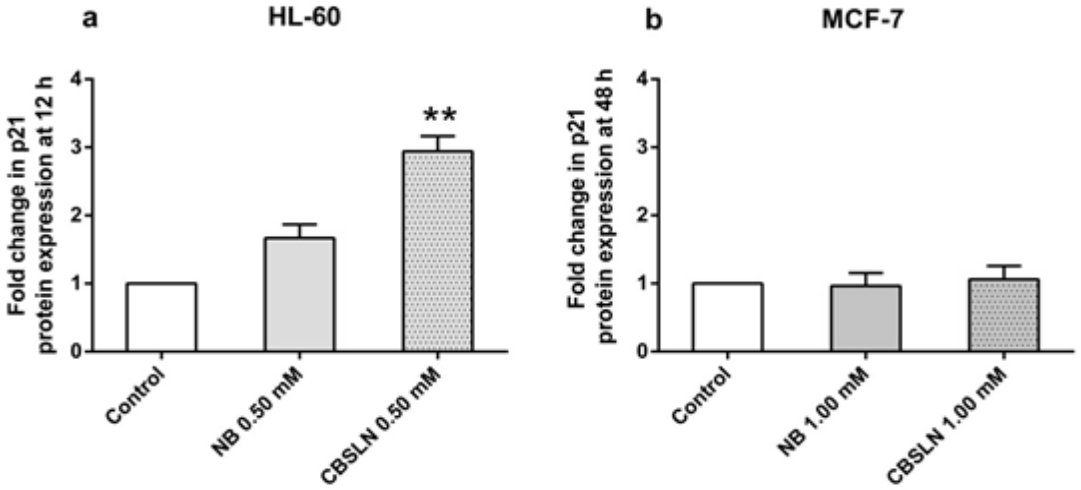

Figure 8. Effects of SLN butyrate delivery on p21 protein expression. Data are presented as fold change compared to that of control cells, i.e. untreated cells. p21 in untreated HL-60 cells was 2626.67 ± 158.41 pg/mL (a) and in MCF-7 untreated cells 4760.00 ± 310.03 pg/mL (b). ** $P < 0.01$ statistical significance versus control cells.

We hypothesized that the different anticancer efficacy of butyrate as CBSLN between HL-60 and MCF-7 cells may be due to differences in the apoptotic mechanisms involved and/or butyrate cellular transport between the two cell lines. First of all, we investigated butyrate activity as NB or CBSLN in each cell line.

In HL-60 cells, NB and CBSLN had different effects on the expression of genes involved in the butyrate mechanism. In particular, NB determined a lesser and earlier mRNA over-expression (Figure 4a) than CBSLN, which determined a marked over-expression at 12 h (Figure 4b). A possible explanation for this might well be the different cell

uptake kinetics as NB or CBSLN, which, in turn, leads to a different transcriptional activity. Of note is that CBSLN induced an up-regulation of *HDAC4* mRNA expression at 12 h in HL-60 cells (Figure 4b) and, at the same time, a significant decrease in total HD activity (Figure 7a).

These data are in line with the hypothesis of a HDI-triggered self-regulatory loop due to a compensatory feedback pathway of HD transcription after inhibition of its enzymatic activity (40). Moreover HL-60 cells are *TP53* null cells and CBSLN induced a marked *CDKN1A* mRNA over-expression both at 6 and 12 h (Figure 4b) and a significant increase in p21 protein expression at 12 h (Figure 8a). In keeping with these data, various studies have reported that butyrate dramatically increases p21 expression in cancer cells, such as osteosarcoma, colon carcinoma, glioma and lung cancer (15). The binding of p21 to the cyclin/cyclin-dependent kinase (CDK) complex is reported to be the main mechanism of butyrate induced inhibition of proliferation, which plays an essential role in G0/G1 arrest. Effectively, it has been reported that p21 forms complexes with cyclin D and CDK 4 or 6 as well as with cyclin E and CDK 2, thus reducing CDK activities and leading to inhibition of G1-S transition (48). Moreover, *CDKN1A* coding for p21 has a specific sequence in its promoter region, which is recognized by the Sp1/Sp3 transcription factors. Indeed, some authors have reported that the butyrate up-regulation of p21 can be explained by selective butyrate regulation of the Sp transcriptional activators, leading to a common mechanism for cell cycle arrest and apoptosis (19, 49).

Our data are in line with several literature reports linking the rise in p21 levels to a histone-direct effect of HDI (14, 22, 50). Butyrate may also modulate other CDK inhibitors, such as p16 coding by *CDKN2A*, whose transcription is up-regulated by CBSLN in HL-60 cells (Figure 4b). This result is in line with Siavoshian's work, where the author reported that treatment of HT-29 with butyrate strongly induces cyclin D and p21 expression, but does not influence *CDK4*, *CDK6* and *P16* expression (51). The butyrate transporter *SLC5A8* was not expressed in HL-60 cells (Figure 6a), whereas the *SLC16A1* transporter was expressed and modulated only by CBSLN (Figure 6b). CBSLN was then able to enhance the butyrate inhibition of HL-60 cell proliferation through a p53 independent pathway as a result of HD inhibition, resulting in marked *CDKN1A* mRNA over-expression and an increase in p21. Therefore, the different butyrate activity in HL-60 cells as CBSLN or NB may be related to butyrate intracellular trafficking improved by SLN, since the active butyrate transporter *SLC5A8* was not expressed.

Figure 5 shows the expression profile of genes involved in the butyrate mechanism of action in MCF-7 cells exposed to NB or CBSLN. Noteworthy is the fact that NB and CBSLN determined up-regulation of the same genes at different time points. There was a general up- regulation trend in the same genes at 48 h for NB and at 24 h for CBSLN. Conversely, NB down-regulated *TP53* transcription, whilst CBSLN up-regulated it. NB led to a significant up-regulation of the mRNA expression of *HDAC4* at 48 h. These data are in line with the slight NB-induced decrease in total HD activity observed in the MCF-7 cells (Figure 7b). Some authors have reported that butyrate inhibits cell proliferation in p53 wild type cancer cells, such as MCF-7, through the p53 pathway. Indeed p53 acetylation precedes the induction of *BAX*, suggesting that p53 mediates NB-induced apoptosis (52-54). Noteworthy was the fact that neither as NB nor as CBSLN was butyrate able to up-regulate *CDKN1A* mRNA expression in MCF-7 cells to such an extent as to induce an increase in p21 protein expression (Figure 8b). Moreover, NB induced a notable up-regulation of the mRNA expression of *BAX* at 48 h. *CDK2* and *CDK4* were significantly down-regulated by NB at 24 h, reaching control level at 48 h. This result is in line with the down-regulation of *CDK4* gene expression in the human non-small lung carcinoma cell line H460 treated with NB (47). Butyrate as NB or CBSLN induced a different modulation of the butyrate transporters *SLC5A8* and *SLC16A1* in MCF-7 cells (Figure 6c and d), i.e., NB-induced *SLC5A8* over-expression at 48 h, while CBSLN induced *SLC16A1* over-expression at the same time point. Hence, the same butyrate activity as CBSLN or NB in MCF-7 cells may be related to the up-regulation of the butyrate active transporters genes *SLC5A8* and *SLC16A1*.

Since the primary target of butyrate may be transcription in both cell lines, CBSLN determined an improved treatment response, as compared to NB, only in HL-60 cells due to the cellular survival/death network. Such findings were also supported by other studies, where low levels of p53 expression are linked to a resistance to HDI (55). Although butyrate's ability to stimulate apoptosis in some adenocarcinoma cells has been well documented, sensitivity to butyrate-induced apoptosis is quite variable and some authors have reported that the

magnitude of p21 protein induction in colon cancer cell lines was smaller in the p53 wild-type cell lines than in the p53 mutant cell lines (20). Indeed, using a retroviral delivery system, an overexpression of p21 in mammary tumor cells led to increased apoptosis (55). Furthermore, some data suggest that histone hyperacetylation is partly responsible for the induction of p21 on colon cancer cell lines, because both butyrate and the specific inhibitor of histone deacetylase as trichostatin A resulted in a similar induction of p21 (56). Moreover, as the ability of butyrate to exert its effects depends on its intracellular concentration, solid lipid nanoparticles may improve butyrate concentration, especially in those cells where active butyrate transporters, such as SLC5A8, are not expressed (e.g., HL-60 cells).

Compared to the hydrogen-coupled transporter SLC16A1, SLC5A8 appears to have an extremely high affinity for butyrate at normal concentrations (25). Moreover, this evidence, along with the fact that SLC5A8 is coupled to a Na^+ concentration gradient, means there is a far greater "push" of butyrate into the cells than with SLC16A1. Indeed, as SLC16A1 relies on an H^+ gradient and as the magnitude of this gradient across the apical membrane is negligible, there is a smaller driving force pushing butyrate across (27). Therefore, the same effects determined by NB and CBSLN in MCF-7 cells may be due to an NB-induced over-expression of *SLC5A8*, which may lead to improved butyrate cellular uptake. Moreover, SLC5A8 butyrate-mediated inhibition of HD has been reported as the underlying mechanism of the tumor-suppressive function of SLC5A8 (25).

CONCLUSION

Delivery of butyrate by solid lipid nanoparticles was able to considerably improve butyrate transcriptional activation in HL-60 cells only, leading to enhanced anticancer activity. According to the mRNA gene expression profile, we hypothesize that the different modulation of gene transcription was due to cell properties such as the expression of *SLC5A8* with different patterns of butyrate internalization as a consequence. Indeed, HL-60 does not express *SLC5A8* (Figure 6a, b), however it was expressed in MCF-7 cells (Figure 6c, d). Therefore, on the basis of these findings, pharmacological enhancement of butyrate transport as solid lipid nanoparticles, according to the specific cancer cell properties, may well represent a useful therapeutic tool in future cancer treatment protocols.

ACKNOWLEDGEMENTS

This work has been supported by the Converging Technologies Research Grant (Nano-IGT Project) from Regione Piemonte, Italy. The authors thank Barbara Wade for her advice on the use of the English language.

REFERENCES

1. Pajak B, Orzechowski A, Gajkowska B. Molecular basis of sodium butyrate-dependent proapoptotic activity in cancer cells. Adv Med Sci. 2007;52:83-8.
2. Goncalves P, Araujo JR, Martel F. Characterization of butyrate uptake by nontransformed intestinal epithelial cell lines. J Membr Biol. 2011;240:35-46.
3. Rahmani M, Dai Y, Grant S. The histone deacetylase inhibitor sodium butyrate interacts synergistically with phorbol myristate acetate (PMA) to induce mitochondrial damage and apoptosis in human myeloid leukemia cells through a tumor necrosis factor-alpha-mediated process. Exp Cell Res. 2002;277:31-47.
4. Chopin V, Slomianny C, Hondermarck H, Le Bourhis X. Synergistic induction of apoptosis in breast cancer cells by cotreatment with butyrate and TNF-alpha, TRAIL, or anti-Fas agonist antibody involves enhancement of death receptors' signaling and requires P21(waf1). Exp Cell Res. 2004;298:560-73.
5. Riggs MG, Whittaker RG, Neumann JR, Ingram VM. n-Butyrate causes histone modification in HeLa and Friend erythroleukaemia cells. Nature. 1977;268:462-4.
6. Sealy L, Chalkley R. The effect of sodium butyrate on histone modification. Cell. 1978;14:115-21.
7. Chen J, Ghazawi FM, Bakkar W, Li Q. Valproic acid and butyrate induce apoptosis in human cancer cells through inhibition of gene expression of Akt/protein kinase B. Mol Cancer. 2006;5:71.
8. Jones PA, Baylin SB. The fundamental role of epigenetic events in cancer. Nat Rev Genet. 2002;3:415-28.
9. Bhalla KN. Epigenetic and chromatin modifiers as targeted therapy of hematologic malignancies. J Clin Oncol. 2005;23:3971-93.
10. Minucci S, Pelicci PG. Histone deacetylase inhibitors and the promise of epigenetic (and more) treatments for cancer. Nat Rev Cancer. 2006;6:38-51.
11. Vousden KH, Lane DP. p53 in health and disease. Nat Rev Mol Cell Biol. 2007;8:275-83.
12. Brown CJ, Lain S, Verma CS, Fersht AR, Lane DP. Awakening guardian angels: drugging the p53 pathway. Nat Rev Cancer. 2009;9:862-73.
13. Lavelle D, Chen YH, Hankewych M, DeSimone J. Histone deacetylase inhibitors increase p21(WAF1) and induce apoptosis of human myeloma cell lines

independent of decreased IL-6 receptor expression. Am J Hematol. 2001;68:170-8.
14. Blagosklonny MV, Robey R, Sackett DL, Du L, Traganos F, Darzynkiewicz Z, et al. Histone deacetylase inhibitors all induce p21 but differentially cause tubulin acetylation, mitotic arrest, and cytotoxicity. Mol Cancer Ther. 2002;1:937-41.
15. Chopin V, Toillon RA, Jouy N, Le Bourhis X. P21(WAF1/CIP1) is dispensable for G1 arrest, but indispensable for apoptosis induced by sodium butyrate in MCF-7 breast cancer cells. Oncogene. 2004;23:21-9.
16. Tonelli R, Sartini R, Fronza R, Freccero F, Franzoni M, Dongiovanni D, et al. G1 cell-cycle arrest and apoptosis by histone deacetylase inhibition in MLL-AF9 acute myeloid leukemia cells is p21 dependent and MLL-AF9 independent. Leukemia. 2006;20:1307-10.
17. Lindemann RK, Gabrielli B, Johnstone RW. Histone-deacetylase inhibitors for the treatment of cancer. Cell Cycle. 2004;3:779-88.
18. Guo F, Sigua C, Tao J, Bali P, George P, Li Y, et al. Cotreatment with histone deacetylase inhibitor LAQ824 enhances Apo-2L/tumor necrosis factor-related apoptosis inducing ligand-induced death inducing signaling complex activity and apoptosis of human acute leukemia cells. Cancer Res. 2004;64:2580-9.
19. Waby JS, Chirakkal H, Yu C, Griffiths GJ, Benson RS, Bingle CD, et al. Sp1 acetylation is associated with loss of DNA binding at promoters associated with cell cycle arrest and cell death in a colon cell line. Mol Cancer. 2010;9:275.
20. Kobayashi N, Kunieda T, Sakaguchi M, Okitsu T, Totsugawa T, Maruyama M, et al. Active expression of p21 facilitates differentiation of immortalized human hepatocytes. Transplant Proc. 2003;35:433-4.
21. Merchant JL, Bai L, Okada M. ZBP-89 mediates butyrate regulation of gene expression. J Nutr. 2003;133(7 Suppl):2456S-60S.
22. Monneret C. Histone deacetylase inhibitors. Eur J Med Chem. 2005;40:1-13.
23. Prince HM, Bishton MJ, Harrison SJ. Clinical studies of histone deacetylase inhibitors. Clin Cancer Res. 2009;15:3958-69.
24. Cuff MA, Shirazi-Beechey SP. The importance of butyrate transport to the regulation of gene expression in the colonic epithelium. Biochem Soc Trans. 2004;32:1100-2.
25. Astbury SM, Corfe BM. Uptake and metabolism of the short-chain fatty acid butyrate, a critical review of the literature. Curr Drug Metab. 2012;13:815-21.
26. Li H, Myeroff L, Smiraglia D, Romero MF, Pretlow TP, Kasturi L, et al. SLC5A8, a sodium transporter, is a tumor suppressor gene silenced by methylation in human colon aberrant crypt foci and cancers. Proc Natl Acad Sci U S A. 2003;100:8412-7.
27. Paroder V, Spencer SR, Paroder M, Arango D, Schwartz S, Jr., Mariadason JM, et al. Na(+)/monocarboxylate transport (SMCT) protein expression correlates with survival in colon cancer: molecular characterization of SMCT. Proc Natl Acad Sci U S A. 2006;103:7270-5.
28. Thangaraju M, Gopal E, Martin PM, Ananth S, Smith SB, Prasad PD, et al. SLC5A8 triggers tumor cell apoptosis through pyruvate-dependent inhibition of histone deacetylases. Cancer Res. 2006;66:11560-4.
29. Heath JR, Davis ME. Nanotechnology and cancer. Annu Rev Med. 2008;59:251-65.
30. Pellizzaro C, Coradini D, Morel S, Ugazio E, Gasco MR, Daidone MG. Cholesteryl butyrate in solid lipid nanospheres as an alternative approach for butyric acid delivery. Anticancer Res. 1999;19:3921-5.
31. Gasco M.R. Solid lipidic nanospheres suitable to a fast internalization into cells. Patent WO 2000030620 A1. 2000
32. Ugazio E, Marengo E, Pellizzaro C, Coradini D, Peira E, Daidone MG, et al. The effect of formulation and concentration of cholesteryl butyrate solid lipid nanospheres (SLN) on NIH-H460 cell proliferation. Eur J Pharm Biopharm. 2001;52:197-202.
33. Brioschi A, Zenga F, Zara GP, Gasco MR, Ducati A, Mauro A. Solid lipid nanoparticles: could they help to improve the efficacy of pharmacologic treatments for brain tumors? Neurol Res. 2007;29:324-30.
34. Salomone B, Ponti R, Gasco MR, Ugazio E, Quaglino P, Osella-Abate S, et al. In vitro effects of cholesteryl butyrate solid lipid nanospheres as a butyric acid pro-drug on melanoma cells: evaluation of antiproliferative activity and apoptosis induction. Clin Exp Metastasis. 2000;18:663-73.
35. Serpe L, Catalano MG, Cavalli R, Ugazio E, Bosco O, Canaparo R, et al. Cytotoxicity of anticancer drugs incorporated in solid lipid nanoparticles on HT-29 colorectal cancer cell line. Eur J Pharm Biopharm. 2004;58:673-80.
36. Serpe L, Laurora S, Pizzimenti S, Ugazio E, Ponti R, Canaparo R, et al. Cholesteryl butyrate solid lipid nanoparticles as a butyric acid pro-drug: effects on cell proliferation, cell-cycle distribution and c-myc expression in human leukemic cells. Anticancer Drugs. 2004;15:525-36.
37. Brioschi A, Zara GP, Calderoni S, Gasco MR, Mauro A. Cholesterylbutyrate solid lipid nanoparticles as a butyric acid prodrug. Molecules. 2008;13:230-54.
38. Minelli R, Serpe L, Pettazzoni P, Minero V, Barrera G, Gigliotti C, et al. Cholesteryl butyrate solid lipid nanoparticles inhibit the adhesion and migration of colon cancer cells. Br J Pharmacol. 2012;166:587-601.
39. Joshi MD, Muller RH. Lipid nanoparticles for parenteral delivery of actives. Eur J Pharm Biopharm. 2009;71:161-72.

40. Souto EB, Muller RH. Lipid nanoparticles: effect on bioavailability and pharmacokinetic changes. Handb Exp Pharmacol. 2010;197:115-41.
41. Bruns T, Peter J, Hagel S, Herrmann A, Stallmach A. The augmented neutrophil respiratory burst in response to Escherichia coli is reduced in liver cirrhosis during infection. Clin Exp Immunol. 2011;164:346-56.
42. Bustin SA, Benes V, Garson JA, Hellemans J, Huggett J, Kubista M, et al. The MIQE guidelines: minimum information for publication of quantitative real-time PCR experiments. Clin Chem. 2009;55:611-22.
43. Mehnert W, Mader K. Solid lipid nanoparticles: production, characterization and applications. Adv Drug Deliv Rev. 2001;47:165-96.
44. Yuan H, Miao J, Du YZ, You J, Hu FQ, Zeng S. Cellular uptake of solid lipid nanoparticles and cytotoxicity of encapsulated paclitaxel in A549 cancer cells. Int J Pharm. 2008;348:137-45.
45. Martins S, Costa-Lima S, Carneiro T, Cordeiro-da-Silva A, Souto EB, Ferreira DC. Solid lipid nanoparticles as intracellular drug transporters: an investigation of the uptake mechanism and pathway. Int J Pharm. 2012;430:216-27.
46. Chopin V, Toillon RA, Jouy N, Le Bourhis X. Sodium butyrate induces P53-independent, Fas-mediated apoptosis in MCF-7 human breast cancer cells. Br J Pharmacol. 2002;135:79-86.
47. Joseph J, Mudduluru G, Antony S, Vashistha S, Ajitkumar P, Somasundaram K. Expression profiling of sodium butyrate (NaB)-treated cells: identification of regulation of genes related to cytokine signaling and cancer metastasis by NaB. Oncogene. 2004;23:6304-15.
48. Sawa H, Murakami H, Ohshima Y, Sugino T, Nakajyo T, Kisanuki T, et al. Histone deacetylase inhibitors such as sodium butyrate and trichostatin A induce apoptosis through an increase of the bcl-2-related protein Bad. Brain Tumor Pathol. 2001;18:109-14.
49. Chirakkal H, Leech SH, Brookes KE, Prais AL, Waby JS, Corfe BM. Upregulation of BAK by butyrate in the colon is associated with increased Sp3 binding. Oncogene. 2006;25:7192-200.
50. Fiskus W, Rao R, Fernandez P, Herger B, Yang Y, Chen J, et al. Molecular and biologic characterization and drug sensitivity of pan-histone deacetylase inhibitor-resistant acute myeloid leukemia cells. Blood. 2008;112:2896-905.
51. Siavoshian S, Blottiere HM, Cherbut C, Galmiche JP. Butyrate stimulates cyclin D and p21 and inhibits cyclin-dependent kinase 2 expression in HT-29 colonic epithelial cells. Biochem Biophys Res Commun. 1997;232:169-72.
52. Bandyopadhyay D, Mishra A, Medrano EE. Overexpression of histone deacetylase 1 confers resistance to sodium butyrate-mediated apoptosis in melanoma cells through a p53-mediated pathway. Cancer Res. 2004;64:7706-10.
53. Harms KL, Chen X. Histone deacetylase 2 modulates p53 transcriptional activities through regulation of p53-DNA binding activity. Cancer Res. 2007;67:3145-52.
54. Palani CD, Beck JF, Sonnemann J. Histone deacetylase inhibitors enhance the anticancer activity of nutlin-3 and induce p53 hyperacetylation and downregulation of MDM2 and MDM4 gene expression. Invest New Drugs. 2012;30:25-36.
55. Condorelli F, Gnemmi I, Vallario A, Genazzani AA, Canonico PL. Inhibitors of histone deacetylase (HDAC) restore the p53 pathway in neuroblastoma cells. Br J Pharmacol. 2008;153:657-68.
56. Archer SY, Meng S, Shei A, Hodin RA. p21(WAF1) is required for butyrate-mediated growth inhibition of human colon cancer cells. Proc Natl Acad Sci U S A. 1998;95:6791-6.